

## Penguin Mediated $B$ Decays at $BABAR$

G. Mancinelli  
University of Cincinnati  
Physics Department  
Cincinnati, OH 45221  
E-mail: *giampi@slac.stanford.edu*  
(for the  $BABAR$  Collaboration)

### Abstract

We report on preliminary results of searches for penguin mediated  $B$  decays based on  $20.7 \text{ fb}^{-1}$  of data collected at the  $\Upsilon(4S)$  peak with the  $BABAR$  detector at PEP-II. The following branching fractions have been measured:  $\mathcal{B}(B^+ \rightarrow \phi K^+) = (7.7_{-1.4}^{+1.6} \pm 0.8) \times 10^{-6}$ ,  $\mathcal{B}(B^0 \rightarrow \phi K^0) = (8.1_{-2.5}^{+3.1} \pm 0.8) \times 10^{-6}$ ,  $\mathcal{B}(B^+ \rightarrow \phi K^{*+}) = (9.7_{-3.4}^{+4.2} \pm 1.7) \times 10^{-6}$ ,  $\mathcal{B}(B^0 \rightarrow \phi K^{*0}) = (8.7_{-2.1}^{+2.5} \pm 1.1) \times 10^{-6}$ ,  $\mathcal{B}(B^+ \rightarrow \omega \pi^+) = (6.6_{-1.8}^{+2.1} \pm 0.7) \times 10^{-6}$ ,  $\mathcal{B}(B \rightarrow \eta K^{*0}) = (19.8_{-5.6}^{+6.5} \pm 1.7) \times 10^{-6}$ , where the first error is statistical and the second systematic. For several other modes we report upper limits on their branching fractions; for example for the following flavor-changing neutral current decays,  $\mathcal{B}(B \rightarrow K l^+ l^-) < 0.6 \times 10^{-6}$ ,  $\mathcal{B}(B \rightarrow K^* l^+ l^-) < 2.5 \times 10^{-6}$ , at 90% Confidence Level (C.L.).

Contributed to the Proceedings of the International Europhysics Conference On High-Energy  
Physics (HEP 2001),  
7/12/2001—7/18/2001, Budapest, Hungary

---

*Stanford Linear Accelerator Center, Stanford University, Stanford, CA 94309*

---

Work supported in part by Department of Energy contract DE-AC03-76SF00515 and NFS grant PHY 9901568.

# 1 Introduction

Flavor-changing neutral currents are forbidden at the tree level in the Standard Model (SM), hence such processes are possible only through penguin loops or suppressed tree amplitudes proportional to small couplings in hadronic flavor mixing (CKM matrix [1]). These rare decays are interesting because their rates and kinematics are in principle sensitive to new heavy particles, predicted for example by supersymmetry models, which can enter the loop. Furthermore, it is possible to use some of these modes to search for direct  $CP$ -violation, measuring the CKM angle  $\beta$  in a penguin environment [2] and compare it with results at the tree level (from the charmonium modes). In the process, we can also test a great number of models just by measuring the branching fractions of penguin mediated  $B$  decays.

The low rates of these decays and their large backgrounds make a high luminosity  $B$ -factory necessary for their searches. The results presented here are derived from  $20.7 \text{ fb}^{-1}$  delivered in 1999 and 2000 by PEP-II [3] at the  $\Upsilon(4S)$  peak and  $2.6 \text{ fb}^{-1}$  off peak (running at  $\sim 40 \text{ MeV}$  below the resonance energy), for a total of  $\sim 22.7$  million  $B\bar{B}$  events. A detailed description of the *BABAR* detector can be found elsewhere [4]. Charge conjugate states are assumed throughout and branching fractions are averaged accordingly.

# 2 Analysis

Much of the background in these rare decays can be reduced by exploiting the good charged particle identification of *BABAR*. This is crucial in analyses involving  $B$  meson decays with no charm in the final state.  $dE/dx$  from the tracking devices provides good  $K/\pi$  separation at  $p < 0.8 \text{ GeV}/c$ , while the response of the internally reflecting ring imaging Cherenkov detector (DIRC) is excellent at higher momenta. Here only the measurement of the Cherenkov angle is used to discriminate  $K$  and  $\pi$  (with better than  $3 \sigma$  separation up to  $3.5 \text{ GeV}/c$ ), while for (lower momentum) composite particle daughters, so-called kaon selectors are used. These selectors combine information from all the relevant subsystems and have typical efficiencies of 80-90% with very low ( $\sim 2$ -3%)  $\pi \rightarrow K$  misidentification probability. The very tight selection criteria applied to electrons give an efficiency of  $\sim 88\%$  with a corresponding  $\pi \rightarrow e$  misidentification probability of  $\sim 0.15\%$ . The typical muon selection efficiency for momenta greater than  $\sim 1 \text{ GeV}/c$  is 60-70%, with  $\pi \rightarrow \mu$  misidentification probability of  $\sim 2\%$ . Performances of particle identification are tested on many control samples kinematically selected from data. Since the backgrounds are dominated by combinatorics from the continuum and since the continuum topology is jetty compared to the isotropic distribution of the signal, event shape variables are exploited to fight this kind of background. The main ones are a Fisher discriminant (already used at CLEO [5]) and the cosine of the angle between the thrust axis of the  $B$  and the rest of the event.

$B$  meson candidates are selected using either the beam energy-substituted mass ( $m_{ES} = \sqrt{(E_{exp})^2 - (p_B)^2}$ , where  $p_B$  is the momentum of the reconstructed  $B$  and  $E_{exp}$  the  $B$  candidate expected energy) or the energy-constrained mass ( $m_{EC}$ , obtained via a kinematic fit of the measured candidate four momentum in the  $\Upsilon(4S)$  frame with the constraint  $E_B^* = E_{beam}^*$ ), and the difference between the reconstructed  $B$  candidate and the beam energies ( $\Delta E = E_B^* - E_{beam}^*$ ), where the stars indicate variables evaluated in the  $\Upsilon(4S)$  rest frame. The latter depends on the mass hypothesis, hence it is a good discriminant for different final states. All analyses use an unbinned maximum likelihood fit to extract the signal yields, while event counting methods are used just as cross checks. Most analyses select their cuts with their signal regions blinded.

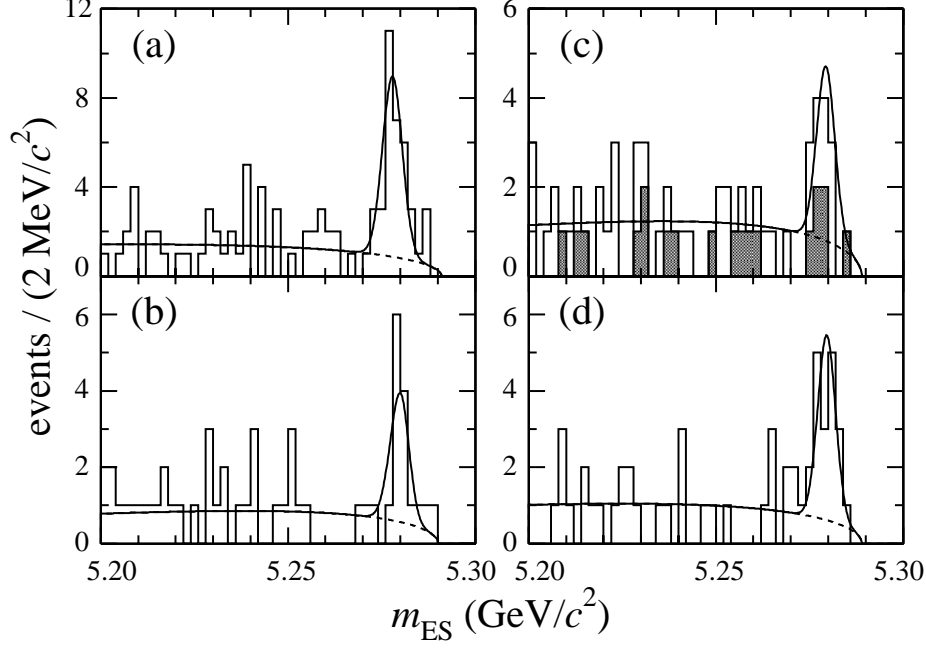


Figure 1: Projections onto the variable  $m_{ES}$ : (a)  $B^+ \rightarrow \phi K^+$ ; (b)  $B^0 \rightarrow \phi K^0$ ; (c)  $B^+ \rightarrow \phi K^{*+}$ ; (d)  $B^0 \rightarrow \phi K^{*0}$ . In (c) the histogram is the sum of the two  $\phi K^{*+}$  channels, with the shaded area corresponding to the  $K^{*+} \rightarrow K_S^0 \pi^+$  decay chain.

## 2.1 $B \rightarrow \phi K^{(*)}$

In the  $B \rightarrow \phi K^{(*)}$  modes we reconstruct the final states  $\phi K^+$ ,  $\phi K^0$ ,  $\phi K^{*+}$  and  $\phi K^{*0}$  where the following intermediate states are recovered:  $K^{*+} \rightarrow K^0 \pi^+$ ,  $K^{*+} \rightarrow K^+ \pi^0$ ,  $K^{*0} \rightarrow K^+ \pi^-$ ,  $\phi \rightarrow K^+ K^-$ ,  $K^0 \rightarrow K_S^0 \rightarrow \pi^+ \pi^-$  and  $\pi^0 \rightarrow \gamma \gamma$ . These decays are particularly interesting because they are dominated by  $b \rightarrow s(d)\bar{s}s$  penguins, with gluonic and electroweak contributions, while other SM contributions are strongly suppressed [6]. In Figure 1 the  $m_{ES}$  distributions for the selected candidates for all the previous modes are shown. The solid (dashed) line shows the PDF projection of the full fit (background only). The fits are mostly for illustration purposes, since the branching fraction results are derived, not from these, but from the maximum likelihood fits. A clear signal is visible in all channels and we report a first observation of the decays  $B^+ \rightarrow \phi K^{*+}$

Decay Mode	Branching Fraction
$B^+ \rightarrow \phi K^+$	$(7.7^{+1.6}_{-1.4} \pm 0.8) \times 10^{-6}$
$B^0 \rightarrow \phi K^0$	$(8.1^{+3.1}_{-2.5} \pm 0.8) \times 10^{-6}$
$B^+ \rightarrow \phi K^{*+}$	$(9.7^{+4.2}_{-3.4} \pm 1.7) \times 10^{-6}$
$B^0 \rightarrow \phi K^{*0}$	$(8.7^{+2.5}_{-2.1} \pm 1.1) \times 10^{-6}$
$B^+ \rightarrow \phi \pi^+$	$< 1.4 \times 10^{-6} @ 90\% \text{ C.L.}$

Table 1: Results of branching fraction measurements for the  $B \rightarrow \phi K^{(*)}$  modes.

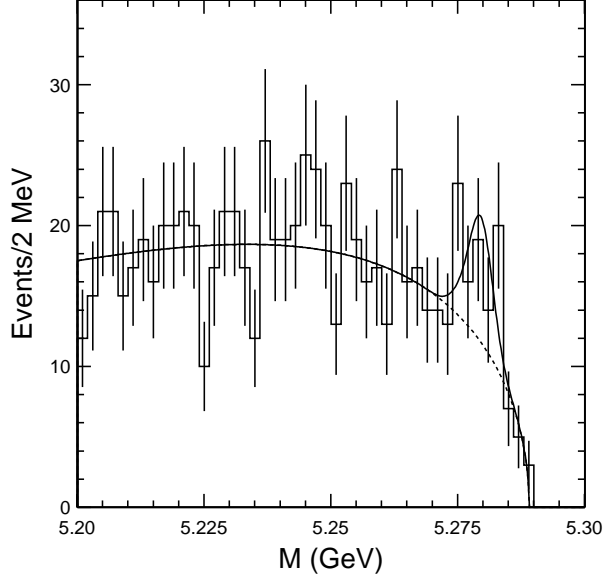


Figure 2: Projections of  $m_{EC}$  for the  $B \rightarrow \omega\pi^+$  mode. The projection is made by selecting events with signal likelihood (computed without  $m_{EC}$ ) exceeding a threshold that optimizes the expected sensitivity.

Decay Mode	Branching Fraction
$B^+ \rightarrow \omega K^+$	$< 4 \times 10^{-6}$ @90% C.L.
$B^+ \rightarrow \omega\pi^+$	$(6.6^{+2.1}_{-1.8} \pm 0.7) \times 10^{-6}$
$B^0 \rightarrow \omega K^0$	$< 14 \times 10^{-6}$ @90% C.L.
$B^0 \rightarrow \omega\pi^0$	$< 4 \times 10^{-6}$ @90% C.L.

Table 2: Results of branching fraction measurements for the  $B \rightarrow \omega X$  modes.

and  $B^0 \rightarrow \phi K^0$ . The final results for these modes are reported in Table 1. They are consistent with previously reported measurements [7] and, within errors, are consistent with isospin invariance under the assumption of penguin diagram dominance.

## 2.2 $B \rightarrow \omega X$

$B$  mesons are reconstructed also in their decays into  $\omega\pi^+$ ,  $\omega\pi^0$ ,  $\omega K^+$ ,  $\omega K_S^0$ , with the  $\omega$  decaying into three pions. A signal is found solely for the mode  $B \rightarrow \omega\pi^+$  (Figure 2) and the branching fraction measurement reported in Table 2 is consistent with those previously reported [8]; in particular we find  $\mathcal{B}(B^+ \rightarrow \omega\pi^+) > \mathcal{B}(B^+ \rightarrow \omega K^+)$ , as expected. Improved upper limits are found for all the other decay channels.

## 2.3 $B \rightarrow \eta K^*$

We have also analyzed the modes  $B \rightarrow \eta K^{*+}$  and  $B \rightarrow \eta K^{*0}$ , where the  $\eta$  decays into two photons, the  $K^{*0}$  into  $K^+\pi^-$ , the  $K^{*+}$  into  $K_S^0\pi^+$  and the  $K_S^0$  into  $\pi^+\pi^-$ . The  $m_{EC}$  projection plot is

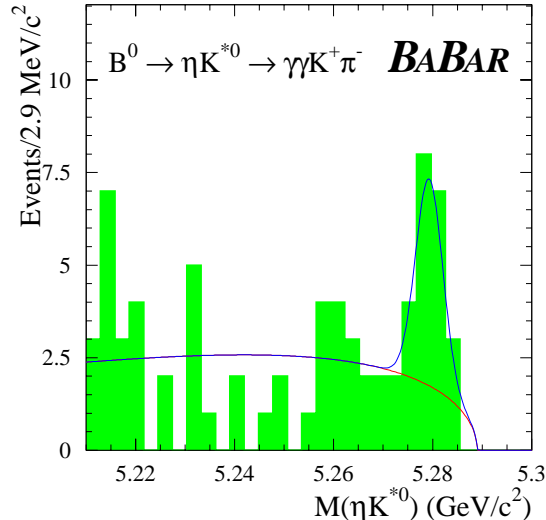


Figure 3:  $B$  candidate invariant mass for  $B^0 \rightarrow \eta K^{*0}$ . The histogram represents data and the smooth curve the fit function.

shown in Figure 3 for the  $\eta K^{*0}$  channel, where a clear signal is present and for which we measure a branching fraction of  $(19.8_{-5.6}^{+6.5} \pm 1.7) \times 10^{-6}$ . We also find an upper limit of  $33.9 \times 10^{-6}$  for the branching fraction of the  $\eta K^{*+}$  mode at 90% C.L. The results are consistent with those previously reported by the CLEO Collaboration [9] and, at least in the  $\eta K^{*0}$  mode, confirm their rather high branching fraction measurement.

## 2.4 $B \rightarrow K^{(*)}l^+l^-$

The dominant contributions for the processes  $B \rightarrow K^{(*)}l^+l^-$  in the SM are the so-called electroweak radiative penguins. These decays have been reconstructed in the modes where  $l = e, \mu$ , the  $K^{*0}$  decays into  $K^+\pi^-$  and the  $K^{*+}$  into  $K_S^0(K_S^0 \rightarrow \pi^+\pi^-)\pi^+$ . These processes have a very clean experimental signature, due to the presence of both a lepton pair and a kaon in the final state.

The main challenge lies in understanding and characterizing the background. To avoid biases as much as possible, a blind analysis is performed, where not only the signal region, but also the sidebands used to determine the background and its normalization, are blinded. Several control samples from data are used to verify the reconstruction efficiencies as determined from Monte Carlo (MC) simulation. In particular  $B \rightarrow J/\psi K^{(*)}$  and  $B \rightarrow \psi(2S)K^{(*)}$  events are used, since they have the same topology as the signal for these modes. Since these decays also constitute a dangerous background, quite complex cuts in the  $\Delta E$  and the lepton pair mass plane are defined to exclude these events, taking into account bremsstrahlung effects; they are shown in Figure 4, where the shaded areas are vetoed. (The same veto is applied to the  $K^*$  modes.) For reference, the two horizontal lines bound the region in which most signal events are found. The charmonium veto removes these backgrounds not only from the signal region, but also from the sideband region, simplifying the description of the background in the fits.

No excess of events in the signal regions is observed, as can be seen in Figure 5, where the  $\Delta E$ ,

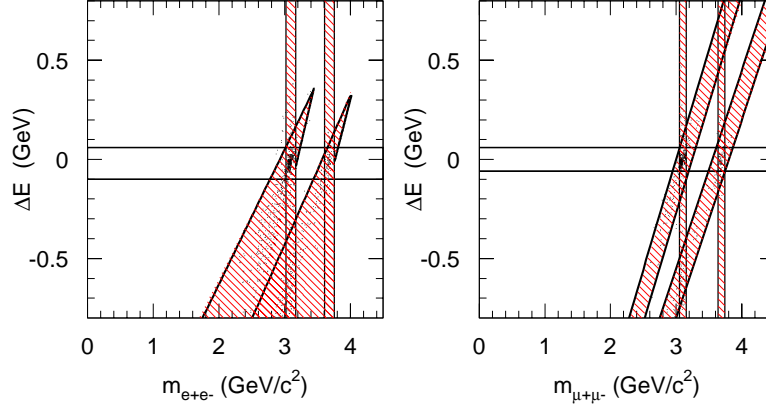


Figure 4: The veto regions in the  $\Delta E$  vs.  $m_{l+l-}$  plane that are populated by  $B \rightarrow J/\psi K$  and  $B \rightarrow \psi(2S)K$  events.

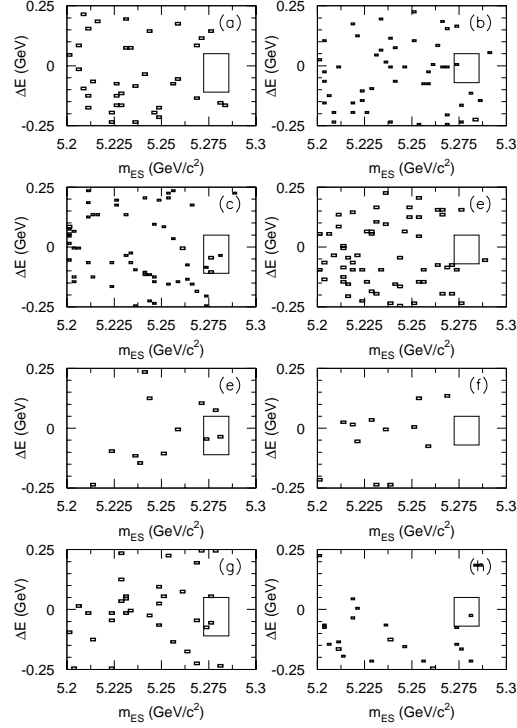


Figure 5: Scatter plots of  $\Delta E$  vs  $m_{ES}$  after all analysis cuts in (a)  $B^+ \rightarrow K^+e^+e^-$ , (b)  $B^+ \rightarrow K + \mu^+\mu^-$ , (c)  $B^0 \rightarrow K^{*0}e^+e^-$ , (d)  $B^0 \rightarrow K^{*0}\mu^+\mu^-$ , (e)  $B^0 \rightarrow K_S^0e^+e^-$ , (f)  $B^0 \rightarrow K_S^0\mu^+\mu^-$ , (g)  $B^+ \rightarrow K^{*+}(\rightarrow K_S^0\pi^+)e^+e^-$ , (h)  $B^+ \rightarrow K^{*+}(\rightarrow K_S^0\pi^+)\mu^+\mu^-$ . The small rectangles indicate the signal region, which is used only for optimizing event selection criteria.

Decay Mode	Branching Fraction upper limits (@90% C.L.)
$B^+ \rightarrow K^+ \mu^+ \mu^-$	$< 1.3 \times 10^{-6}$
$B^+ \rightarrow K^+ e^+ e^-$	$< 0.9 \times 10^{-6}$
$B^0 \rightarrow K^0 \mu^+ \mu^-$	$< 4.5 \times 10^{-6}$
$B^0 \rightarrow K^0 e^+ e^-$	$< 4.7 \times 10^{-6}$
$B \rightarrow K l^+ l^-$	$< 0.6 \times 10^{-6}$
$B^0 \rightarrow K^{*0} \mu^+ \mu^-$	$< 3.6 \times 10^{-6}$
$B^0 \rightarrow K^{*0} e^+ e^-$	$< 5.0 \times 10^{-6}$
$B^+ \rightarrow K^{*+} \mu^+ \mu^-$	$< 17.5 \times 10^{-6}$
$B^+ \rightarrow K^{*+} e^+ e^-$	$< 10.0 \times 10^{-6}$
$B \rightarrow K^* l^+ l^-$	$< 2.5 \times 10^{-6}$

Table 3: Results of branching fraction measurements for the  $B \rightarrow K^{(*)} l^+ l^-$  modes.

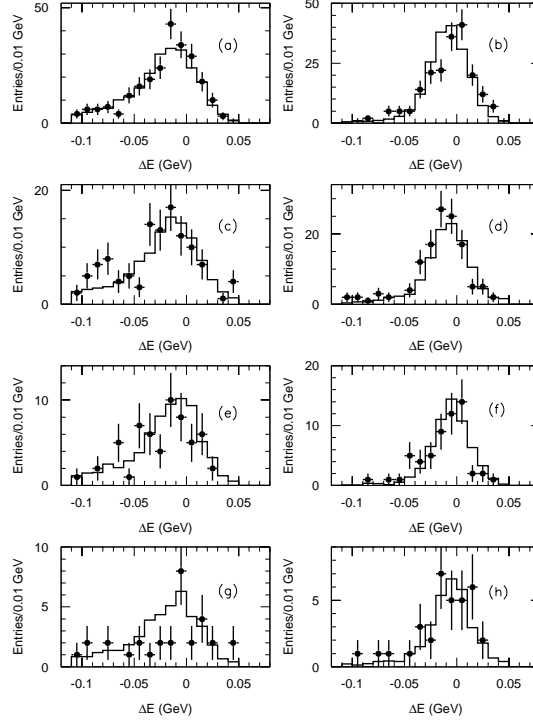


Figure 6: Comparison of  $\Delta E$  shapes in several data control samples: (a)  $B^+ \rightarrow J/\psi(\rightarrow e^+ e^-) K^+$ , (b)  $B^+ \rightarrow J/\psi(\rightarrow \mu^+ \mu^-) K^+$ , (c)  $B^0 \rightarrow J/\psi(\rightarrow e^+ e^-) K^{*0}$ , (d)  $B^0 \rightarrow J/\psi(\rightarrow \mu^+ \mu^-) K^{*0}$ , (e)  $B^0 \rightarrow J/\psi(\rightarrow e^+ e^-) K_S^0$ , (f)  $B^0 \rightarrow J/\psi(\rightarrow \mu^+ \mu^-) K_S^0$ , (g)  $B^+ \rightarrow J/\psi(\rightarrow e^+ e^-) K^{*+}(\rightarrow K_S^0 \pi^+)$ , (h)  $B^+ \rightarrow J/\psi(\rightarrow \mu^+ \mu^-) K^{*+}(\rightarrow K_S^0 \pi^+)$ . The normalization is absolute.

$m_{ES}$  scatter plots are shown for all decay modes. Very low level of background is present. As a cross check, after removing the  $J/\psi$ ,  $\psi(2S)$  veto, we repeat the analysis on the  $J/\psi ll$  and  $\psi(2S)ll$  control samples. Not only is a clear signal found, but the resulting  $\Delta E$  shapes and normalizations are in very good agreement with the simulation, as shown in Figure 6, where the points with error bars show the on-resonance data, and the solid histograms the predictions of the charmonium MC simulation. All the analysis selection criteria have been applied except for the charmonium veto, which is reversed. The results are shown in Table 3. The combined limits for  $B \rightarrow K^{(*)}ll$  are now very close to the theoretical expectations for the SM [10] and represent a significant improvement over previous results [11] [12] [13].

### 3 Summary

With about 23 millions  $B\bar{B}$  events *BABAR* has already very interesting results on penguin mediated decays. We have reported the first observation of the decays  $B^+ \rightarrow \phi K^{*+}$  and  $B^0 \rightarrow \phi K^0$  for which we found the branching fractions  $(9.7^{+4.2}_{-3.4} \pm 1.7) \times 10^{-6}$  and  $(8.1^{+3.1}_{-2.5} \pm 0.8) \times 10^{-6}$  respectively, and the upper limit set on the  $\mathcal{B}(B \rightarrow Kll)$ ,  $< 0.6 \times 10^{-6}$ , is very close to the theoretical expectations for the SM. Other branching fractions have been measured for penguin mediated  $B$  decays:  $\mathcal{B}(B^+ \rightarrow \phi K^+) = (7.7^{+1.6}_{-1.4} \pm 0.8) \times 10^{-6}$ ,  $\mathcal{B}(B^0 \rightarrow \phi K^{*0}) = (8.7^{+2.5}_{-2.1} \pm 1.1) \times 10^{-6}$ ,  $\mathcal{B}(B^+ \rightarrow \omega \pi^+) = (6.6^{+2.1}_{-1.8} \pm 0.7) \times 10^{-6}$ ,  $\mathcal{B}(B \rightarrow \eta K^{*0}) = (19.8^{+6.5}_{-5.6} \pm 1.7) \times 10^{-6}$ .

### 4 Acknowledgments

We are grateful to our PEP-II colleagues for their painstaking dedication and tireless effort, which has made possible the achievement of excellent luminosity and, consequently, the results presented here. The collaborating institutions wish to thank SLAC for its support and kind hospitality.

### References

- [1] N. Cabibbo, Phys. Rev. Lett. **10** (531) 1963; M. Kobayashi and T. Maskawa, Prog. Theor. Phys. **49** (652) 1973.
- [2] I. Dunietz and J.L. Rosner, Phys. Rev. **D 34** (1404) 1986.
- [3] PEP-II Conceptual Design Report, SLAC Report No. 418 1993.
- [4] *BABAR* Collaboration, B. Aubert *et al.*, SLAC-PUB-8569, submitted to Nucl.Instrum.Meth.
- [5] CLEO Collaboration, D.M. Asner *et al.*, Phys. Rev. **D 53** (1039) 1996.
- [6] N.G. Deshpande and J. Trampetic, Phys. Rev. **D 41** (895) 1990; N.G. Deshpande and X.-G. He, Phys. Lett. B **336** 471 1994; R. Fleischer, Z. Phys. C **62** 811 1994.
- [7] CLEO Collaboration, R.A. Briere *et al.*, Phys. Rev. Lett. **86** (3718) 2001.
- [8] CLEO Collaboration, C.P. Jessop *et al.*, Phys. Rev. Lett. **85** (2881) 2000.
- [9] CLEO Collaboration, S.J. Richichi *et al.*, Phys. Rev. Lett. **85** (520) 2000.
- [10] A. Ali *et al.*, Phys. Rev. **D 61** (074024) 2000.

- [11] CDF Collaboration, T. Affolder *et al.*, Phys. Rev. Lett. **83** (3378) 1999.
- [12] CLEO Collaboration, S. Anderson *et al.*, submitted to Phys. Rev. Lett.; hep-ex/1006060.
- [13] T. Iijima for the Belle Collaboration, to appear in the Proceedings of the 4th International Conference on B physics and  $CP$ - Violation, Ago Town, Mie Prefecture, Japan, February 19-23 (2001); hep-ex/0105005.